FEATURE

SAR TOMOGRAPHY: AN ADVANCED TOOL FOR 4D SPACEBORNE RADAR SCANNING WITH APPLICATION TO IMAGING AND MONITORING OF CITIES AND SINGLE BUILDINGS

G. Fornaro[1], Senior Member IEEE, A. Pauciullo[1], D. Reale[1] Member IEEE,
X. Zhu[2,3] Member IEEE, and R. Bamler[2,3] Fellow IEEE
[1]Institute for the Electromagnetic Sensing of the Environment (IREA), National Research Council (CNR) 80124 Napoli, Italy (e-mail: fornaro.g@irea.cnr.it, pauciullo.a@irea.cnr.it, reale.d@irea.cnr.it).
[2]Remote Sensing Technology Institute (IMF), German Aerospace Center (DLR), 82234 Oberpfaffenhofen (xiao.zhu@dlr.de, richard.bamler@dlr.de).
[3]Technische Universität München, Lehrstuhl für Methodik der Fernerkundung, 80333 Munich, Germany.

1. Introduction

Synthetic Aperture Radar (SAR) has become a routine geo-information source complementing optical imagery. The microwaves used by SAR can penetrate canopy, soil, snow and ice allowing for estimation of volumetric properties, e.g. biomass. SAR also can employ polarization for deriving structural parameters of objects [1] [2]. Another strong and unique selling point of SAR is that surface displacements and object deformations can be measured to mm-level accuracy by exploiting multitemporal acquisitions. In particular, the recent technological advancement in SAR systems has provided very high resolution (VHR) X-Band sensors, such as the TerraSAR-X/TanDEM-X mission and the Cosmo-Skymed constellation, characterized by spatial resolutions of the order of 1 meter. With respect to the former generation of medium resolution (a ten, or a few tens of meters) C-Band SAR systems, the increase of the resolution of such sensors allows much higher details of ground structures to be captured.

On the downside we have to cope with an imaging geometry that does not support an easy interpretation of SAR images, especially in complex scenarios. A single SAR image is the projection of the 3D scene into the azimuth (x) – range (r) coordinates. Whenever only surface scattering is present and the local slopes of the surfaces are smaller than the local incidence angle this mapping is injective: in this case the image can be easily converted to any other map projection. However, for volumetric scatterers (e.g. forests) and steep – or even vertical – surfaces, like in urban areas, SAR imaging becomes non-injective and real 3D imaging is required.

SAR Tomography (TomoSAR) is a technique that allows resolving scatterer densities in the *third* native radar co-ordinate "elevation (s)" (also referred to as slant–height, orthogonal to the azimuth-range plane). It extends the synthetic aperture principle – as used in the azimuth direction – also to the elevation direction by exploiting multiple passes of the radar at slightly different orbit positions to establish a virtual array of antennas, as depicted in Figure 1. The synthetic aperture in elevation allows reducing the width of the elevation antenna beam providing a fine beam "radar scanner" from the space able to generate high resolution 3D images, hence the additional name of 3D Imaging.

The inherent (Rayleigh) elevation resolution ρ_s of the tomographic arrangement is related to the spread Δb of this array [3]–[6]:

$$\rho_s = \frac{\lambda_r}{2\Delta b} \tag{1}$$

and can reach values of the order of a few meters.

By stacking all the multiview coherent images and by performing the tomographic processing, s-profiles can be

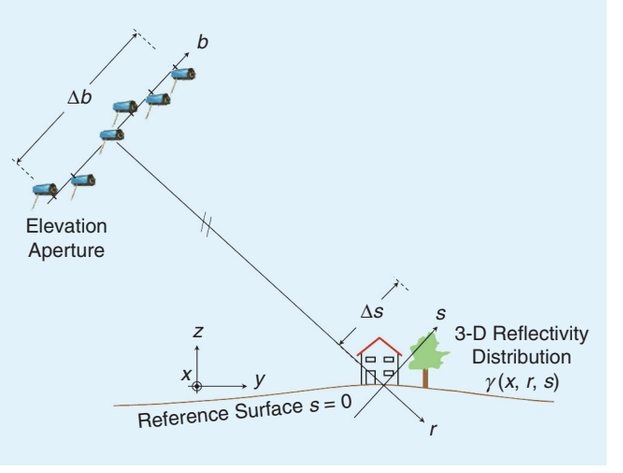

Figure 1. TomoSAR geometry

retrieved for every x–r pixel. These profiles can be continuous in the case of forest biomass imaging [3] or may consist only of a few discrete scatterers, typically corresponding to scatterers located on the ground, facade and roof, in the case of urban mapping. This article is devoted to the latter application.

Since the elevation antenna array is in the far-field of the imaged objects, the complex signal received at any of the radar positions b_n is a sample of the Fourier transform of the reflectivity profile in elevation $\gamma(s)$:

$$g_n = \int_{\Delta s} \gamma(s)\exp(-j2\pi\xi_n s)ds, \qquad n=1,\ldots,N \tag{2}$$

where $\xi_n = -2b_n/(\lambda r)$ is the spatial (elevation) frequency. Therefore, retrieval of the s-profile is framed as a spectral estimation problem and reliable scatterers showing a good degree of coherence can be identified by looking for the peaks in the focused reflectivity function.

Since the multipass dataset is acquired at different time instants, sometimes over a period of years, possible motion and deformation of objects must be additionally considered in the process of estimation of the s-profiles, either as useful information (subsidence, tectonics, landslides, etc.) or simply as nuisance parameters. Space/velocity (4D) imaging techniques, also known as Differential SAR Tomography (D-TomoSAR), extends the 3D imaging and can be applied to measure also the deformation parameters (velocity spectrum) of any temporal coherent scatterer in the focused 3D space [7][8][6]. If motion is considered, eq. is in fact extended to a 2D or even higher dimensional Fourier transform, depending on how many motion modes are accounted for (e.g. linear, periodic, thermal, etc.) [7]–[10]. In this case the technique is referred to as Multi-Dimensional (MD) SAR imaging. Finally, the possibility of screening the reflectivity function in elevation allows discriminating the presence of multiple peaks, even exhibiting different velocities, and hence solve the interference and increase the density of monitored scatterers [8][11][6].

MD imaging (MDI) is in effect a technique that extends the Persistent Scatterer Interferometry (PSI) [12]–[15] approach. PSI assumes the presence of a dominant scattering mechanism in each pixel and therefore cannot resolve the layover problem. Moreover, theoretical and experimental results on both simulated and real data have shown [16] that the use of an imaging approach (i.e. SAR Tomography), which exploits the phase as well as the amplitude information, performs better even in the detection of dominant persistent scatterers and in the estimation of their localization and deformation parameters with respect to classical PSI which uses only the phase information.

2. Tomographic SAR Inversion Algorithms

In the following for sake of simplicity we refer to the 3D reconstruction case. Discretizing the elevation profile in eq. leads to this standard linear system equation:

$$\mathbf{g} = \mathbf{R}\gamma + \boldsymbol{\varepsilon} \tag{3}$$

where $\mathbf{g}$ is the vector of measurements according to eq. (2), $\boldsymbol{\gamma}$ is the elevation profile, $\mathbf{R}$ is the irregular Fourier matrix composed of the so-called steering vectors and $\boldsymbol{\varepsilon}$ is noise.

The spectral estimation problem of s-profile reconstruction can be framed as the inversion of this linear system. The inversion must be carefully implemented because: (i) the Fourier samples are irregularly spaced at ξ_n, (ii) their number N may be small, (iii) the SNR may be low for the majority of the pixels, (iv) the data may contain non-Gaussian phase noise due to uncompensated atmospheric delay and unmodeled motion and (v) the orbit tube of modern SAR satellites is tight leading to a small Δb and, hence, to a low elevation resolution. Many different MDI algorithms have been proposed in the recent literature to cope with these problems.

The simplest algorithm is based on the Beam-Forming (BF) that is the matched filter, i.e., $\hat{\boldsymbol{\gamma}} = \mathbf{R}^H\mathbf{g}$. It computes the amount of backscattered energy at different elevations by digitally steering (through the column vectors of $\mathbf{R}$) the beam of the multibaseline array. Because of the irregular acquisition distribution BF reconstruction exhibits poor performances in terms of large sidelobes and also it does not allow exceeding the Rayleigh resolution of eq. (1) [5].

To overcome such limitations, advanced inversion approaches have been proposed in the literature. The need to achieve super-resolution involves a discretization that exceeds the Rayleigh limit thus making the problem in (3) underdetermined. A class of super-resolution TomoSAR algorithms is based on regularized inversion and tries to find the solution among the infinitely many solutions of the underdetermined system model by minimizing:

$$\hat{\boldsymbol{\gamma}} = \arg\min_{\gamma}\{\|\mathbf{g}-\mathbf{R}\gamma\|_2^2 + \beta\,\|\boldsymbol{\Gamma}\boldsymbol{\gamma}\|_p^q\} \tag{4}$$

A rather simple and easily to be implemented solution is based on the use of the Singular Value Decomposition (SVD) *regularized* linear inversion [5][6]. In this case, Tikhonov (Wiener) filtering choices of the singular values allow achieving the solution to the problem in (4) with $\beta = \sqrt{SNR}$, $\boldsymbol{\Gamma} = \mathbf{I}$ and $p = 2$ and $q = 2$ [6]. Another solution strictly related to the above approach is based on Truncated SVD: in this case $\beta = 0$ and a hard limitation of the singular values is used [5] to control the ill-conditioning nature of the inversion. Super-resolution can be achieved by reducing the scene support with respect to the theoretical limit given by $\Delta s = \lambda r/(2\tilde{b})$, where $\tilde{b}$ is the average baseline separation, and controlling the inversion by choosing a suitable number of singular values during the inversion process, provided that the noise level is sufficiently low. SVD achieves typically also better sidelobe suppression than plain BF [5][6].

For many acquisition configurations SVD super-resolution is not sufficient. The orbits of TerraSAR-X, e.g., are controlled

so accurately that Δb is typically in the order of 250–350 m leading to an elevation resolution of 30–50 m, which is unacceptably large compared to the range and azimuth resolutions of 1–3 m. The classical super-resolving spectral estimators that are used for TomoSAR are adaptive beam-forming (CAPON) [17] (non-linear, non-parametric) or MUSIC and ESPRIT (both non-linear, parametric) [18][19]. The latter parametric methods do not retrieve continuous *s*-profiles but rather estimate the positions of individual scatterers. They need the number of scatterers as prior information. These methods are computationally fast. However, they require the estimation of covariance matrices which is usually done by multilooking and reduces the azimuth and range resolution. In the case of two or more scatterers these estimators are not efficient, i.e. they do not reach the Cramér-Rao Lower Bound. They are also not energy conserving and the strength of the estimated spectral lines are not straightforwardly related to the reflectivity of the scatterer.

The optimum parametric method – under Gaussian noise assumption – is the non-linear least-squares estimator. However, it would require a combinatorial search of scatterer positions. Here the theory of Compressive Sensing (CS) comes into play.

CS is able to reconstruct sparse signals from their irregularly sampled Fourier transform in a quasi-parametric way. Indeed the elevation profiles of urban objects usually contain only a few scatterers, e.g. one at the ground and one on the façade. Since the elevation resolution ρ_s from eq. (1) is often much worse than the range resolution, the elevation extent of these scatterers is much smaller than ρ_s, rendering these scatterers *discrete*. These are the very prerequisites for using the theory of sparse signal reconstruction and CS. By referring to (4), CS allows finding the solution by selecting $\beta = \beta_K$, $\mathbf{\Gamma} = \mathbf{I}$ and $p = q = 1$, where K is the number of sparse targets [20]. The first CS TomoSAR simulations were presented in [21] and the SR capability of CS for TomoSAR reconstruction and its robustness on elevation estimation against phase noise have been proven in [22]. To overcome the drawbacks of a simple CS estimator, the "Scale-down by L1 norm Minimization, Model selection, and Estimation Reconstruction" (SL1MMER) algorithm has been proposed in [23][24], a spectral estimation algorithm based on CS, with an additional model order selection and final maximum likelihood parameter estimation.

As a last remark it is important to point out that not only estimation of motion parameters (e.g., velocity, topography, etc.) associated with scatterers interfering in the same pixel can be achieved, but also separation of time series is possible by adoption of proper tomographic based filtering techniques. Results of experiments with real data have confirmed this peculiarity of MDI data processing [11].

3. Application Examples

The advanced processing via MDI of VHR X-Band data allows nowadays increasing the density of monitored scatterers dramatically compared to PSI. As a consequence, precise monitoring of even single buildings and in general of infrastructures as well as cultural heritage is possible. In the following, experiments on X-Band data acquired by both the TerraSAR-X and Cosmo-Skymed sensors are discussed. Processing is carried out with implementation of MDI at IREA-CNR and DLR-IMF.

3.1. MDI Systems of IREA-CNR and DLR-IMF

3.1.1. MDI system of IREA-CNR

The MDI approach developed in the last few years at IREA-CNR exploits a simple tomographic processing based on beam-forming to estimate the backscattering distribution in the elevation/velocity domain (4D MDI) and to identify scatterers (up to two), possibly interfering within the same image pixel [25]. The algorithm separates the problem in two steps: the first step is devoted to estimate the scatterers parameters, i.e. the position in space and deformation, whereas the second step concerns the selection of the number of scatterers in a detection framework, i.e., paying attention to achieve high detection performance for a given false alarm rate. Particularly, the selection stage exploits a detection scheme which is based on the sequential use of a detector based on the Generalized Likelihood Ratio Test for single scatterers in [13][16] .

The MDI technique developed in IREA has demonstrated, for the first time, the capability of this processing approach to resolve multiple scatterers interfering in the same pixel by using C-Band data in [26]: further significant results on C-Band data were reported in [8] and [11]. Nevertheless, the first demonstration of the capability of MDI to resolve distributed layover occurring over vertical structures as buildings have been shown in [32]: in this case the MDI beam-forming tomographic processing was applied to a dataset of TerraSAR-X data acquired over the area of Las Vegas. Particularly relevant were in this case the results achieved over the Mirage hotel which are not shown here for brevity.

In order to face the higher sensitivity of X-Band radiation to small changes of targets, such as those caused by thermal dilation, MDI processing has been extended to measure even this component in the 5D domain (space/velocity + thermal dilation). In fact, even if already observed in C-Band (ERS and Envisat) data [28][29], this effect is much more evident in X-Band data due to the increase of sensitivity associated with the shorter wavelength [30]–[32]. To account also for the thermal dilation component, the deformation model, typically made of the linear temporal term, is extended with a new one, measured in mm/K, which is linearly related to the temperature of the area at the acquisition instants [10].

3.1.2. MDI system of DLR-IMF: Tomo-GENESIS

The workhorse of interferometric processing at DLR is the GENESIS system [33]. It has been the basis for the

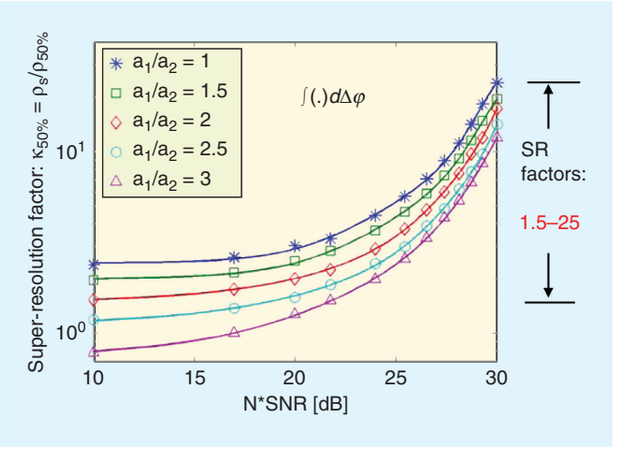

Figure 2. Fundamental bound of super-resolution (SR): SR factor of the SL1MMER algorithm as a function of N SNR under different amplitude ratios a_1/a_2 of two close scatterers [24].

developments of DLR's operational SRTM and TanDEM-X processors. An extended version of it (PSI-GENESIS) handles PSI processing of medium resolution data, wide-swath mosaics as well as very high resolution spotlight data. During the last years several new algorithms for TomoSAR processing have been developed at DLR extending the system to what we introduce as "Tomo-GENESIS" [34].

The layover phenomenon in a SAR image of an urban area is mainly caused by the following two scenarios: (i) buildings with different heights in layover with the ground or (ii) taller building in layover with the ground and the roof of a lower building. Both scenarios suggest that double scatterer pairs with smaller elevation distances will be more frequent than those with larger distances. Therefore, SR is crucial for VHR tomographic SAR reconstruction in urban environment. This makes super-resolving TomoSAR algorithms particularly important for urban mapping.

The SL1MMER algorithm is demonstrated to be an efficient estimator and achieves super-resolution factors of 1.5~25 at the interesting parameter range for TomoSAR (see Figure 2), i.e. N = 10~100 and SNR = 0~10 dB [22][23]. The results shown in Figure 3 are approximately applicable to nonlinear least-squares estimation as well, and hence, although it is derived experimentally, they can be considered as a fundamental bound for SR of spectral estimators. In [24] the super-resolution capability of the SL1MMER algorithm is demonstrated using TerraSAR-X data.

For an input data stack, the Tomo-GENESIS system retrieves the following information: number of scatterers inside a pixel, amplitude and phase, topography and motion parameters (e.g. linear deformation velocity and amplitude of thermal dilation induced seasonal motion) of each detected scatterer. Compared to other existing MDI processing systems, it has the following new features: the time warp method for multi-component nonlinear motion estimation [9]; the CS based SL1MMER algorithm and super-resolution capability [22]–[24]; fusion of PSI and TomoSAR processing for operational purpose [35]; RANSAC based point cloud fusion algorithm [36][35]. Currently, the system is extending for object reconstruction from the unstructured TomoSAR point clouds [37].

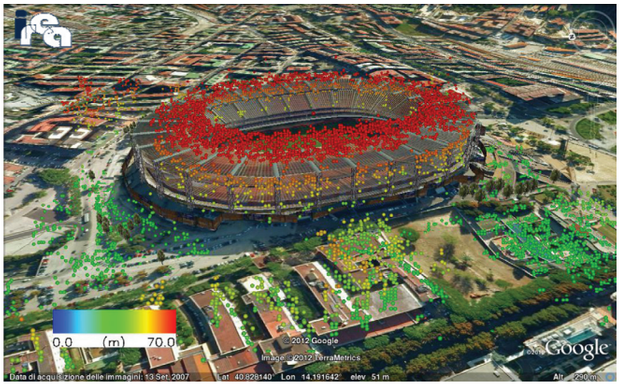

Figure 3. 3D view of the San Paolo Stadium, Naples, Italy, reconstructed by the 5D MDI with COSMO/SKYMED data provided by the Italian Space Agency. Colormap is set according to the estimated height [30]–[32].

3.2. Application Examples

3.2.1. Space radar scanning with SAR tomography

To show the capabilities of MDI to achieve "synthetic" radar scanning for imaging ground structures we present the following results relevant to the San Paolo Stadium in the city of Naples, Italy. A dataset of 28 images acquired by the Cosmo-Skymed constellation on descending passes in the standard stripmap mode (~3 m spatial resolution) from February 2010 to February 2011 were processed with the 5D MDI algorithm. Figure 3 shows the three-dimensional reconstruction of the stadium visualized on a Google Earth map: the colors are set according to the estimated height. Note that even in this moderate resolution mode a large density of targets compared to PSI is achieved, especially on the roof [30]–[32].

3.2.2. Compressed Sensing SAR Tomography for super resolution spaceborne radar scanners

Figure 4 presents a 3D view of the single buildings visualized in GoogleEarth reconstructed by SL1MMER using a stack of 25 TerraSAR-X images [24]. The test building is the Bellagio hotel at downtown Las Vegas. Compared to PSI, TomoSAR offers in general a tremendous improvement in detailed reconstruction and monitoring of urban areas. Experiments using TerraSAR-X high resolution spotlight data stacks show the scatterer density to be in the order of 600,000~1,000,000/km^2 compared to a PS density in the

order of 40,000~100,000 PS/km^2 [34][38]. In particular, together with its SR power, SL1MMER provides ultimate information one can retrieve from the data stack. Figure 5 presents the number of scatterers map obtained by SVD-Wiener inversion (left) and SL1MMER (right) over the test area where blue indicates zero scatterers inside the azimuth-range pixel, green stands for one and red for two. Non-parametric estimators can only detect two scatterers with an elevation distance larger than approximately the Rayleigh elevation resolution unit ρ_s. Therefore, it is not surprising that the double scatterers detected by the linear estimator are mainly located on the upper part of the building façade. The result of SL1MMER shows a much denser red color which indicates a larger amount of detected double scatterers. For an urban area like this typically about 30~40% of the scatterers detected by SL1MMER are double scatterers compared to less 10~20% detected by linear estimators.

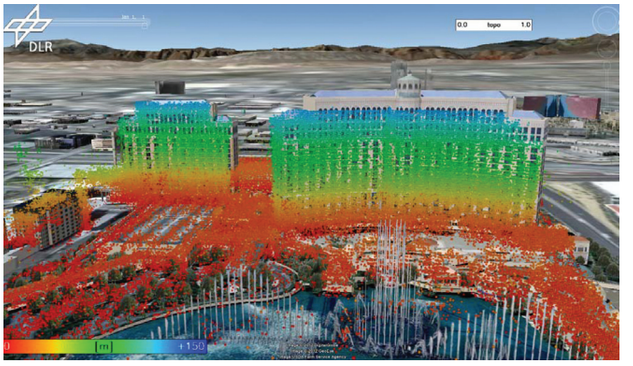

Figure 4. 3D view of the single building visualized in GoogleEarth reconstructed by SL1MMER using a stack of 25 TerraSAR-X images (the color represents height) [24].

3.2.3. TomoSAR point cloud fusion

Due to the side-looking geometry of SAR, a single stack of SAR images only provides information on one side of a building. To serve the function of urban structure monitoring, fusion of the TomoSAR results of multiple stacks from different view angles can provide us with a shadow-free point cloud with high degree of coverage over the entire urban area.

At the test site of Berlin, we have a luxury data archive with a large number of TerraSAR-X high resolution spotlight images including a stack of 94 SAR images from ascending orbit and another stack of 79 SAR images from descending orbit are processed. For both stacks, the acquisition time span is about four years. Figure 6 present the 3D positions of the fused point clouds. From Figure 6 Figure 6: small structures like the Victory Column, i.e. the statue at the center of the park can be easily identified. For this test-site, about 40 million scatterers are detected from the two data stacks.

3.2.4. Multicomponent motion estimation

D-TomoSAR was originally proposed in [7] for estimating linear motion of multiple scatterers inside a pixel. Motion,

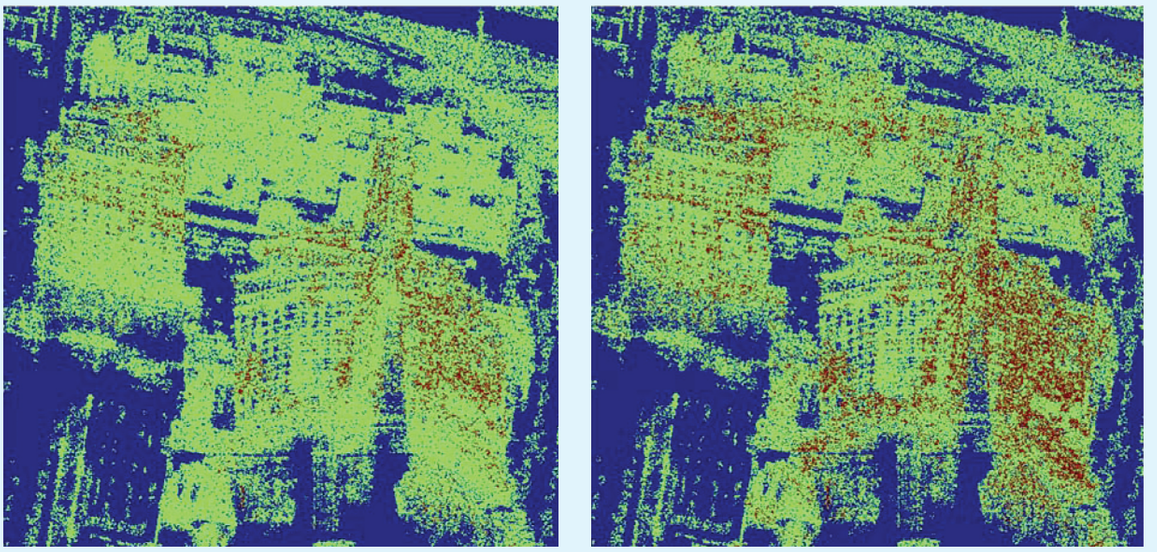

Figure 5. Double scatterer density for SVD-Wiener (a) and SL1MMER (b) reconstruction (Blue: Null scatterers per pixel; Green: Single; Red: Double) [24]. The superresolution capability of SL1MMER leads to more detected double scatterers, in particular at the lower parts of the facades.

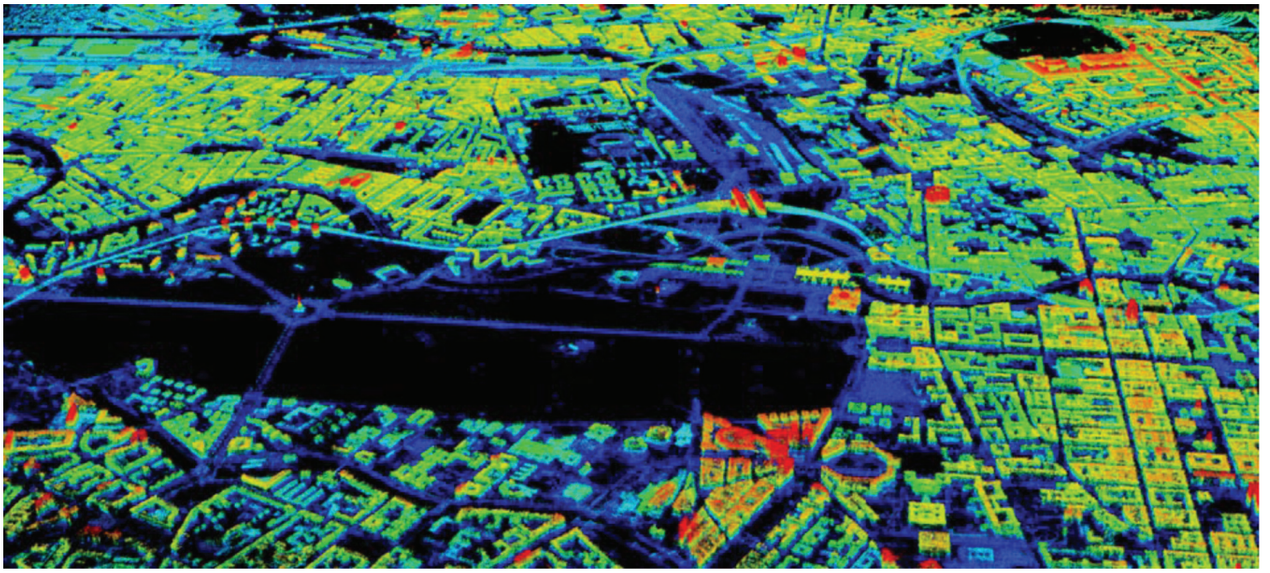

Figure 6. Fusion of two point clouds generated from TerraSAR-X data stacks of ascending and descending orbit. The color represents height [35].

however, is often nonlinear (periodic, accelerating, stepwise, etc.). Conventional D-TomoSAR has been extended to estimate multicomponent nonlinear motion in [9] by proposing the generalized "time warp" method. It rewrites the D-TomoSAR system model to an M+1-dimensional standard spectral estimation problem, where M indicates the user defined motion model order and, hence, enables the motion estimation for all possible complex motion models.

Figure 7 shows an example of multicomponent motion estimation. Since July 2009, the selected area over Las Vegas (see Figure 7a) is undergoing a pronounced subsidence centered at the convention center. Together with the thermal dilation induced seasonal motion of the metallic building structure, the selected area is characterized by a two-component nonlinear motion. Here, we choose the motion basis function as a sine function with a period of one year for seasonal motion and linear function for linear subsidence. And hence the motion parameters to be estimated are amplitude of seasonal motion and linear deformation velocity. The final estimation results of the generalized time-warp method are presented in Figure 7 including elevation estimates in meter (b), amplitude of seasonal motion in millimeter (c) and the LOS linear deformation velocity in millimeter/year (d).

If we know the temperature at the time of data acquisitions, we can also accordingly choose the temperature as the basis function to model thermal dilation induced deformation [10] [30][31]. In this case, the thermal coefficient is estimated that represents the strength of undergoing thermal dilation induced deformation. An example is presented in Figure 8. The site under investigation is relevant to the area of the Bellagio hotel and casino (see Figure 4). Figure 8(a) shows in the native radar geometry (range and azimuth are the horizontal and vertical directions, respectively), the topography retrieved by the MDI Beam-Forming imaging approach by using only single scatterers. Figure 8(b) and 8(c) show the estimated topography and thermal dilation with single and double scatterers by using the 5D Beam-Forming imaging: note that thermal dilation mostly affects the outer parts of building and exhibits different behavior on the same building according to the different projection of thermal dilation along the radar line-of-sight.

4. Conclusion and Further Developments

With reference to the current status of VHR tomographic SAR inversion presented in this article, the following conclusions can be drawn:

- VHR tomographic SAR inversion is able to reconstruct the shape and motion of individual buildings and entire city areas.
- Super-resolution is crucial and possible for VHR tomographic SAR inversion for urban infrastructure.
- TomoSAR reconstruction from *multiple* tracks enables us to reconstruct the complete structure of individual buildings and to generate 3D point clouds of the illuminated area with a point density comparable to LiDAR
- The motion or deformation of buildings is often nonlinear (periodic, accelerating, stepwise, etc.). This is particularly true with VHR SAR data. Multicomponent nonlinear motion of multiple scatterers can be separated and further estimated by tomographic reconstruction.

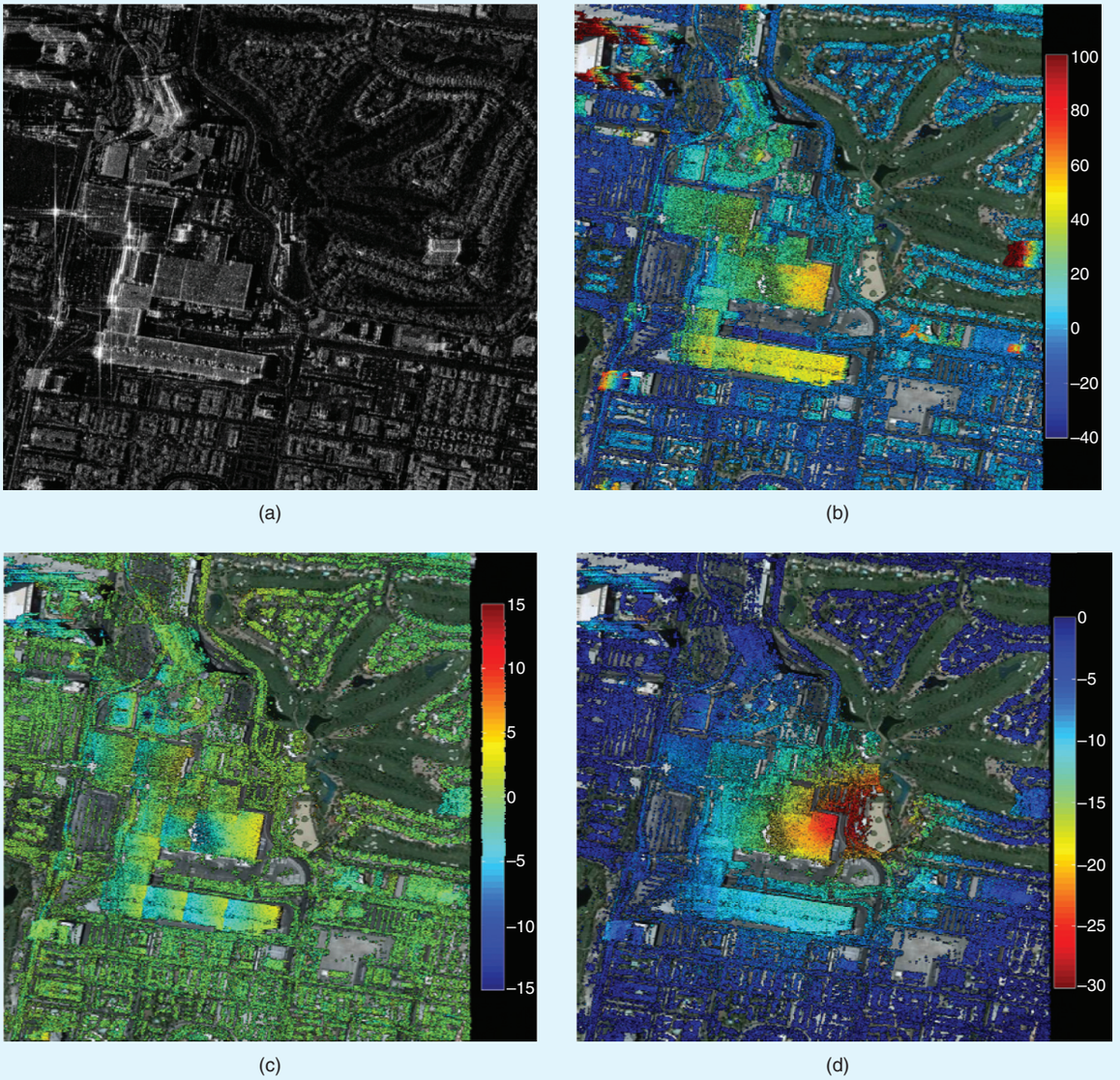

Figure 7. TomoSAR estimates of the selected area in Las Vegas: TerraSAR-X intensity map (a); Elevation estimates (b; unit: m) amplitude of seasonal motion (c; unit: mm) and linear deformation velocity (d; unit: mm/y) [9].

A few topics for further study are outlined which mainly concern 1) tomographic SAR reconstruction from mixed single-pass/multipass data stacks 2) object reconstruction from TomoSAR point clouds.

- Tomographic SAR reconstruction from mixed single-pass/repeat-pass data stacks:
  So far, the data used for spaceborne VHR tomographic SAR inversion are repeat-pass data stacks. With TanDEM-X, for the first time there is a real multi-antenna array system in space. It enables us to acquire data pairs simultaneously and repeatedly in time. The TanDEM-X data pairs are free of motion, atmosphere and temporal decorrelation and, hence, possess much higher data quality. The fusion of TerraSAR-X and TanDEM-X data, i.e. adding a couple of TanDEM-X acquisition pairs to the TerraSAR-X data stacks, can be used to improve the result of tomographic SAR inversion on the one hand, and to explore the limits of tomographic reconstruction on the other hand [39].

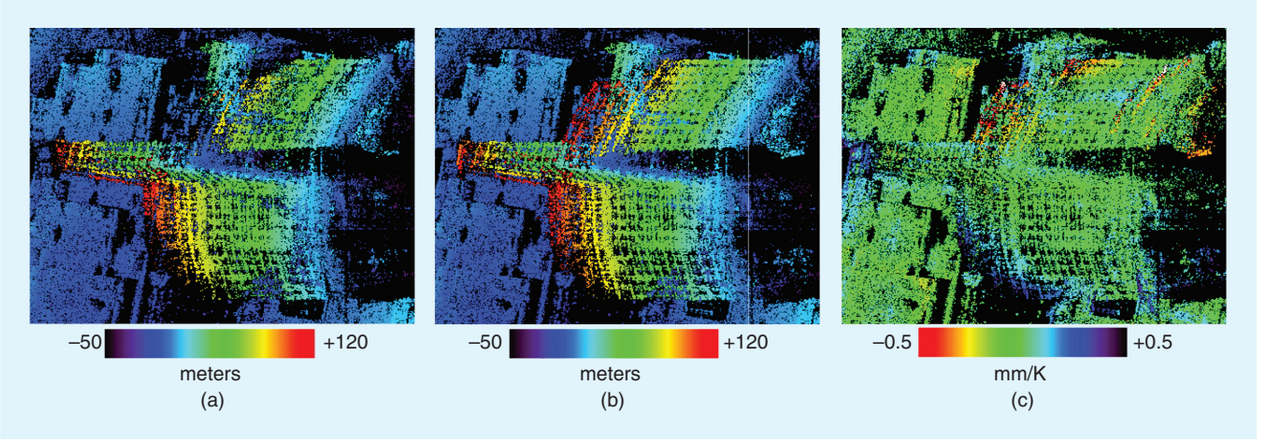

Figure 8. Thermal dilation analysis with TerraSAR-X data. (a) estimated topography with the 4D imaging (single scatterers); (b) estimated topography with the 5D imaging (single and double); (c) estimated thermal coefficients with the 5D imaging (single and double) [10][30][31].

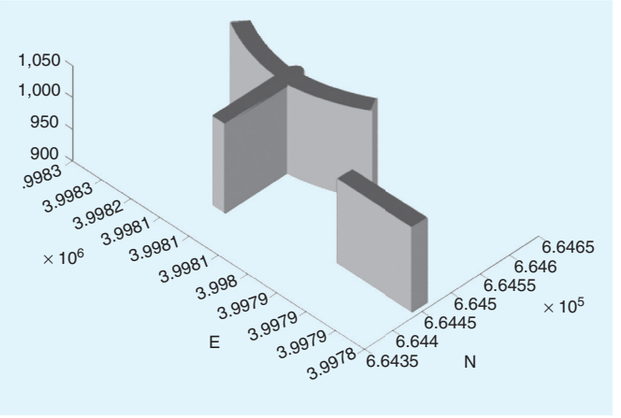

Figure 9. From TomoSAR point clouds to objects: reconstructed building façade of the test building Bellagio hotel in Las Vegas [37].

- Object reconstruction from TomoSAR point clouds: These tomographic point clouds can be potentially used for building façade reconstruction in urban environment from space with some special considerations such as side-looking geometry, anisotropic estimation accuracy and decorrelation. Yet in order to provide a high quality spatio-temporal 4D city model, object reconstruction from these TomoSAR point clouds is emergent. A 3D view of the reconstructed façades over a test building Bellagio hotel in Las Vegas (see Figure 4) using point clouds from multiple viewing angles, i.e. both ascending and descending orbits, is exemplified in Figure 9.

References

[1] J.C. Curlander and R.McDonough, "Synthetic Aperture Radar – System and Signal Processing", New York, John Wiley & Sons, Inc , 1991.

[2] G. Franceschetti and R. Lanari, "Synthetic Aperture Radar Processing", CRC Press, Boca Raton FL, 1999.

[3] A. Reigber and A. Moreira, "First demonstration of airborne SAR tomography using multibaseline L-band data", *IEEE Trans. Geosci. Remote Sens.*, vol. 38, no. 5, pp. 2142–2152, Sep. 2000.

[4] F. Gini, F. Lombardini, and M. Montanari, "Layover solution in multibaseline SAR interferometry", *IEEE Trans. Aerosp. Electron. Syst.*, vol. 38, no. 4, pp. 1344–1356, Oct. 2002.

[5] G. Fornaro, F. Serafino, and F. Soldovieri, "Three-dimensional focusing with multipass SAR data", *IEEE Trans. Geosci. Remote Sens.*, vol. 41, no. 3, pp. 507–517, Mar. 2003.

[6] X. Zhu and R. Bamler, "Very High Resolution Spaceborne SAR Tomography in Urban Environment," *IEEE Trans. Geosci. Remote Sens.*, vol. 48, no. 12, pp. 4296–4308, Dec. 2010.

[7] F. Lombardini, "Differential tomography: A new framework for SAR interferometry," *IEEE Trans. Geosci. Remote Sens.*, vol. 43, no. 1, pp. 37–44, Jan. 2005.

[8] G. Fornaro, D. Reale, and F. Serafino, "Four-dimensional SAR imaging for height estimation and monitoring of single and double scatterers", *IEEE Trans. Geosci. Remote Sens.*, vol. 47, no. 1, pp. 224–237, Jan. 2009.

[9] X. Zhu, and R. Bamler, "Let's Do the Time Warp: Multicomponent Nonlinear Motion Estimation in Differential SAR Tomography," *IEEE Geosci. Remote Sens. Lett.*, vol. 8, no. 4, pp. 735–739, July 2011.

[10] D. Reale, G. Fornaro, and A. Pauciullo, Extension of 4D SAR Imaging to the Monitoring of Thermally Dilating Scatterers, *IEEE Trans. Geosci. Remote Sens.,* accepted for publication.
[11] G. Fornaro, F. Serafino, and D. Reale, "4D SAR imaging: The case study of Rome," *IEEE Geosci. Remote Sens. Lett.*, vol. 7, no. 2, pp. 236–240, Apr. 2010.
[12] A. Ferretti, C. Prati, and F. Rocca, "Nonlinear Subsidence Rate Estimation Using Permanent Scatterers in Differential SAR Interferometry", *IEEE Trans. Geosci. Remote Sens.*, vol 38, pp. 2202–2212, 2000.
[13] A. Ferretti, C. Prati, and F. Rocca, "Permanent Scatterers in SAR Interferometry", *IEEE Trans. Geosci. Remote Sens.*, vol. 39, no. 1, pp. 8–20, Jan. 2001.
[14] N. Adam, R. Bamler, M. Eineder, B. Kampes, Parametric estimation and model selection based on amplitude-only data in ps-interferometry. In: Proceedings of FRINGE, 2005.
[15] B. Kampes, Radar interferometry: persistent scatterer technique. Springer, 2006.
[16] A. De Maio, G. Fornaro, A. Pauciullo, "Detection of Single Scatterers in Multi-Dimensional SAR Imaging", *IEEE Trans. Geosci. Remote Sens.*, vol. 47, no. 7, July 2009.
[17] F. Lombardini, F. Gini, P. Matteucci, "Application of array processing techniques to multibaseline InSAR for layover solution", *Proc. of the 2001 IEEE Radar Conf.*, pp. 210–215, 2001.
[18] F. Gini, F. Lombardini, "Multilook APES for multibaseline SAR interferometry," *IEEE Trans. on Signal Processing*, 50 (7): 1800–1803, 2002.
[19] M. Nannini, R. Scheiber, A. Moreira, Estimation of the minimum number of tracks for SAR tomography. *IEEE Trans. Geosci. Remote Sens.* 47 (2): 531–543, 2009.
[20] A. Budillon, A. Evangelista, A.; and G. Schirinzi, "Three-Dimensional SAR Focusing From Multipass Signals Using Compressive Sampling", *IEEE Trans. Geosci. Remote Sens.*, 49(1), 488–499, 2011.
[21] A. Budillon, A. Evangelista, G. Schirinzi, "SAR Tomography from sparse samples," *Proc. IEEE 2010 IGARSS Conf.*, Cape Town, Africa, 2010.
[22] X. Zhu, R. Bamler, Tomographic SAR Inversion by L1 Norm Regularization – The Compressive Sensing Approach, *IEEE Trans. Geosci. Remote Sens.*, 48(10), pp. 3839–3846, 2010.
[23] X. Zhu, R. Bamler, "Super-Resolution Power and Robustness of Compressive Sensing for Spectral Estimation with Application to Spaceborne Tomographic SAR," *IEEE Trans. Geosci. Remote Sens.*, 50(1), pp. 247–258, 2012.
[24] X. Zhu, R. Bamler, "Demonstration of Super-resolution for Tomographic SAR Imaging in Urban Environment," *IEEE Trans. Geosci. Remote Sens.,* 50(8), pp. 3150–3157, 2012.
[25] A. Pauciullo, D. Reale, A. De Maio, G. Fornaro, "Detection of Double Scatterers in SAR Tomography," *IEEE Trans. Geosci. Remote Sens.*, vol. 50, no. 9, Sept. 2012.
[26] G. Fornaro, F. Serafino, "Imaging of Single and Double Scatterers in Urban Areas via SAR Tomography", *IEEE Trans. Geosci. Remote Sens*, 44(12), pp. 3497–3505, 2006.
[27] D. Perissin and F. Rocca "High-Accuracy Urban DEM Using Permanent Scatterers", *IEEE Trans. Geosci. Remote Sens.*, vol. 44, no. 11, pp. 3338–3347, Nov. 2006.
[28] D. Perissin and A. Ferretti, "Urban-Target Recognition by Means of Repeated Spaceborne SAR Images", *IEEE Trans. Geosci. Remote Sens.*, vol. 45, no. 12, pp. 4043–4058, Dec. 2007.
[29] O. Monserrat, M. Crosetto, M. Cuevas, and B. Crippa, "The Thermal Expansion Component of Persistent Scatterer Interferometry Observations," *IEEE Geosci. Remote Sens. Letters*, vol. 8, no. 5, pp. 864–868, Sept. 2011.
[30] G. Fornaro, D. Reale, and S. Verde, "Potential of SAR for Monitoring Transportation Infrastructures: an Analysis with the Multi-Dimensional Imaging Technique," *J. Geophys. Eng.* 9 S1, 2012, doi:10.1088/1742-2132/9/4/S1.
[31] G. Fornaro, D. Reale, and S. Verde, "Bridge Thermal Dilation Monitoring With Millimeter Sensitivity via Multidimensional SAR Imaging," *IEEE Geosci. Remote Sens. Lett.*, early access article, doi: 10.1109/LGRS.2012.2218214.
[32] D. Reale, G. Fornaro, A. Pauciullo, X.Zhu, and R. Bamler, "Tomographic Imaging and Monitoring of Buildings With Very High Resolution SAR Data," *IEEE Geosci. Remote Sens. Letters*, vol. 8, no.4, pp. 661–665, July 2011.
[33] N. Adam, B. Kampes, M. Eineder, J. Worawattanamateekul, M. Kircher, The development of a scientific permanent scatterer system, ISPRS Hannover Workshop, Hannover, 2003.
[34] X. Zhu, Very High Resolution Tomographic SAR Inversion for Urban Infrastructure Monitoring – A Sparse and Nonlinear Tour, Deutsche Geodätische Kommission, Reihe C, Nr. 666, Verlag der Bayerischen Akademie der Wissenschaften, ISBN 978-3-7696-5078-5, 2011.
[35] Y. Wang, X. Zhu, Y. Shi., R. Bamler, "Operational TomoSAR Processing Using TerraSAR-X High Resolution Spotlight Stacks from Multiple View Angles", *Proc. IEEE 2012 IGARSS Conf.*, Munich, Germany, 2012.
[36] S. Gernhardt, X. Cong, M. Eineder, S. Hinz, & R. Bamler, Geometrical Fusion of Multitrack PS Point Clouds IEEE Geoscience and Remote Sensing Letters, Vol. 9 (1), pp. 38–42, 2012.
[37] X. Zhu, M. Shahzad, R. Bamler, From TomoSAR Point Clouds to Objects: Façade Reconstruction, *Proc. TyWRRS 2012*, Naples, Italy, 2012.
[38] S. Gernhardt, N. Adam, M. Eineder, and R. Bamler, "Potential of Very High Resolution SAR for Persistent Scatterer Interferometry in Urban Areas," *Ann. GIS*, vol. 16, no. 2, pp. 103–111, Jun. 2010.
[39] X. Zhu, R. Bamler, "Sparse Tomographic SAR Reconstruction from Mixed TerraSAR-X/TanDEM-X Data Stacks," *Proc. IEEE 2012 IGARSS Conf*, Munich, Germany, 2012.